ECOHYDROLOGY
Ecohydrol. **5**, 1–18 (2012)
Published online 11 November 2010 in Wiley Online Library
(wileyonlinelibrary.com) DOI: 10.1002/eco.177

Significant variation in vegetation characteristics and dynamics from ecohydrological optimality of net carbon profit

Stefan C. Dekker,[1]* Jasper A. Vrugt,[2,3,4] and Rebecca J. Elkington[1]

[1] *Department of Environmental Sciences, Utrecht University, PO BOX 80115, 3508 TC Utrecht, The Netherlands*
[2] *Department of Civil and Environmental Engineering, University of California, Irvine, CA 92697, USA*
[3] *Institute for Biodiversity and Ecosystem Dynamics, University of Amsterdam, Nieuwe Achtergracht 166, 1018 WV Amsterdam, The Netherlands*
[4] *Earth and Environmental Sciences Division, Los Alamos National Laboratory, Mail Stop T003, Los Alamos, NM 87545, USA*

ABSTRACT

Recent contributions to the ecological literature have questioned the continued usefulness of the classical model calibration paradigm in estimating parameters in coupled ecohydrological models. Schymanski (2007) and Schymanski *et al*. (2007, 2008) have demonstrated that the assumption of vegetation optimality precludes the need for site-specific data for estimating vegetation properties, transpiration fluxes, and CO_2 assimilation. The goal of this article is twofold. We first show that significant advances in optimality-based vegetation modelling can be made if we embrace a novel concept of stochastic optimization that includes explicit recognition of parameter uncertainty. We adapted the original Vegetation Optimality Model (VOM) to a multi-layer soil and canopy vegetation optimality model, VOM_{mlsc} with dynamically varying throughfall fraction. The DiffeRential Evolution Adaptive Metropolis (DREAM) algorithm is used to find parameter values with high values of net carbon profit (NCP), a proxy for biological fitness. We then show that significant variability exists in optimized vegetation properties and primarily transpiration fluxes from optimality of NCP. Seemingly, a myriad of vegetation species is possible that results in optimal values of NCP. Using data from a Douglas-fir plantation in The Netherlands, we found relative poor correspondence between modelled and measured ET and CO_2-fluxes. The fitting of these two fluxes and values of the model parameters can be much improved when VOM_{mlsc} is calibrated directly against these respective observations. Yet, the NCP values derived this way deviate considerably from their maximum possible value. This challenges the appropriateness of current weights to aggregate the various carbon costs and benefits into a single NCP scalar. Copyright © 2010 John Wiley & Sons, Ltd.

KEY WORDS soil moisture dynamics; gas exchange; photosynthesis; optimality principle; net carbon profit; leaf area index; DiffeRential Evolution Adaptive Metropolis; eddy correlation measurements; Markov Chain Monte Carlo simulation; Douglas-fir

Received 19 March 2010; Accepted 7 October 2010

Abbreviations NCP, net carbon profit; MCMC, Markov Chain Monte Carlo; DREAM, DiffeRential Evolution Adaptive Metropolis; VOM, Vegetation Optimality Model; VOM_{mlsc}, multi-layer soil and canopy VOM model; LAI, leaf area index.

INTRODUCTION AND SCOPE

The exchange of water and carbon between the vegetation and the ambient atmosphere is of great importance in many scientific disciplines, including plant physiology, ecology, meteorology, hydrology, and soil science, and is currently receiving a surge of attention within the context of climate change. Many different vegetation models have been developed in the past few decades to help understand and predict spatial and temporal dynamics in CO_2 and H_2O fluxes between the vegetation and the atmosphere. These models range from simple empirical-based regression equations to more complicated stochastic approaches and increasingly complex physically based models. This last category of models typically use multiple layers to represent the canopy, and explicitly take into account the radiation distribution and turbulent exchange within the vegetation to simulate the detailed behaviour of the stomata of individual leaves. These models have become the fundamental tools to study stomatal behaviour, and the exchange of CO_2 and H_2O between vegetation and the atmosphere.

Irrespective of the complexity of these coupled transpiration and carbon uptake models, they all contain parameters whose values cannot be measured directly in the field, but can only be meaningfully derived through calibration against site-specific data. This generally requires detailed physiological measurements of the vegetation, and observations of CO_2 and H_2O fluxes above the canopy using 15- or 30-min covariances of vertical wind speed, atmospheric water vapour density, and carbon dioxide. Unfortunately, these observations typically require significant human commitment, and are rather expensive. Moreover,

* Correspondence to: Stefan C. Dekker, Department of Environmental Sciences, Utrecht University, PO BOX 80115, 3508 TC Utrecht, The Netherlands. E-mail: s.dekker@geo.uu.nl

the validity of coupled ecohydrological models outside the range of measurements for which they have been calibrated cannot be guaranteed (Dekker *et al*., 2000; Schymanski *et al*., 2008). For example, increasingly large prediction errors are usually observed outside the calibration period. Finally, plant communities adapt dynamically to varying environmental conditions, but are assumed to take on fixed behaviour within this classical calibration framework (Schymanski *et al*., 2008). There is therefore a pressing need for ecohydrological parameter estimation approaches that do not rely on excessive and expensive calibration data sets of historical fluxes and states, and allow continuous vegetation adaptation to changing environmental conditions.

The hypothesis of vegetation optimality provides an attractive and parsimonious alternative to using detailed site-specific measurements for ecohydrological model calibration. This approach allows for dynamically varying ecohydrological parameters, and therefore provides more detail and accuracy in modelling vegetation dynamics and behaviour.

The assumption that self-organization of biological systems is governed by some principles of optimal adaptation has long been implicit in biological thinking (Sutherland, 2005). However, the use of optimality principles in behavioural modelling has been subject to considerable debate, especially within biological literature. Reynolds and Chen (1996) criticized the hypothesis of optimality because of the difficulty in defining an objective criteria that properly accounts for the natural variability in plants, presence of significant model simplifications, and absence of a definite time integral in which plants foresee changes to their environment. Nevertheless, Kull (2002) and Kleidon (2007) argue that any mismatch between model predictions and reality simply indicates that the 'true' underlying plant optimization strategy has not yet been found, and that the objective function to be maximized has yet to be discovered.

Eagleson (1978) promoted the idea of optimality in vegetation modelling from an ecohydrological perspective. One of the objective functions he defined, the maximization of soil moisture and thus minimization of evapotranspiration, was later established to be unrealistic as this would also result in the minimization of photosynthetic activity (Kerkhoff *et al*., 2004). Rodriguez-Iturbe *et al*. (1999) proposed that individuals in a plant community would act together to minimize water stress, but this approach did not allow for predictions of an optimal composition of the vegetation for given climatic conditions. Makela *et al*. (1996) constrained that evaporation must be less than rainfall.

Around the same time as Eagleson's seminal work, Cowan and Farquhar (1977) were approaching optimality modelling from an ecophysiological perspective and assumed that plants would dynamically optimize their stomatal conductivity to maximize total photosynthesis for given transpiration amounts. Unfortunately, this approach is only appropriate for short time intervals, because changes in leaf area and water balance dynamics are ignored. The maximization of net primary production (NPP) is another objective that has found widespread use as the defining mechanism governing the response of plants in optimality-based models. NPP refers to gross primary production, which equals the total amount of carbon assimilated by plants, minus autotrophic respiration (Roxburgh *et al*., 2005), irrespective of whether this energy is subsequently available to the plants or not. The maximization of net carbon profit (NCP) is, for this reason, considered by at least some researchers to be a more appropriate objective function than the maximization of NPP (Schymanski, 2007; Schymanski *et al*., 2007). NCP only refers to the energy that is available to the plants for increasing their biological fitness. NCP can be seen as unallocated carbon, whereas NPP is carbon that already is allocated for wood production.

Recent contributions to the ecohydrological literature have shown that the principle of vegetation optimality of NCP provides accurate predictions of daily to annual transpiration and CO_2 fluxes between the canopy and ambient atmosphere (Schymanski, 2007; Schymanski *et al*., 2007, 2008, 2009). These initial results inspire confidence in the use of NCP for analysing and understanding vegetation structure and dynamics for given soil and environmental conditions, and predicting the response of vegetation, and hence the functioning of ecosystems in the face of climatic change. Yet, the main focus of this research has been on finding a single combination of parameter values that maximizes the respective optimality criteria used. For example, Schymanski (2007) and Schymanski *et al*. (2007, 2009) used the shuffled complex evolution (SCE-UA) global optimization algorithm to optimize vegetation properties using NCP under given environmental conditions. This approach downplays variability and essentially ignores model and forcing data uncertainty. Furthermore, our experience with highly parameterized ecohydrological models suggests that significant parameter interaction and dispersion exist from observations of water and carbon exchange. In this article, we therefore argue that significant advances in the field of Vegetation Optimality Modelling (VOM) can be made if we embrace a concept of stochastic optimization that includes explicit recognition of parameter uncertainty. A distribution of 'optimal' parameter values is more appropriate in light of natural variability and uncertainty, and contains important diagnostic information about the model and optimality criteria used.

The purpose of this study is to exhaustively explore the parameter space of the VOM model of Schymanski (2007) and Schymanski *et al*. (2007, 2009), and demonstrate significant dispersion of vegetation characteristics by optimality of NCP. To illustrate our ideas, we extend the original VOM approach of Schymanski (2007) and Schymanski *et al*. (2007) to include a multi-layer canopy and time-varying throughfall fraction. The use of a single 'big-leaf' may be appropriate for vegetation with a low leaf area index (LAI) (Schymanski *et al*., 2009), but

DOI: 10.1002/eco

there are doubts as to whether it can represent vegetation properties and dynamics at high LAI (Acock *et al.*, 1978).

The extended VOM model, hereafter referred to as VOM with multi-layer soil and canopy (VOM_{mlsc}), is then applied to a Douglas-fir stand in The Netherlands, where NCP is maximized. In our optimality analysis, we consider six different parameters that represent the most important static and dynamically varying vegetation properties of VOM_{mlsc}. These parameters are estimated using the DiffeRential Evolution Adaptive Metropolis (DREAM) Markov Chain Monte Carlo (MCMC) algorithm with NCP as optimality criteria. This MCMC scheme, recently developed by Vrugt *et al.* (2009a,b), is especially designed to efficiently search the parameter space for multiple optimal solutions. The outcome of DREAM is used to analyse VOM_{mlsc} parameter uncertainty and compare the marginal distribution of simulated plant transpiration, CO_2 uptake, and soil moisture dynamics in the rooting zone with observations of these respective quantities using eddy correlation and time domain reflectometry (TDR) measurements.

The remainder of this article is organized as follows. In the Section on Vegetation Optimality Model, we present the coupled soil water balance, ecophysiological gas exchange, and the photosynthesis model, referred to as VOM_{mlsc}. The Section on Study Site and Measurements describes the experimental study site in The Netherlands, and field measurements used to evaluate the predictions of plant transpiration, CO_2 assimilation, and soil moisture dynamics of VOM_{mlsc}. In the Section on Optimization Strategy of VOM_{mlsc}, we describe in short the DREAM algorithm to efficiently explore the parameter space for high NCP values, and the Section on Results presents the results and marginal distributions of our optimality analysis. Here, we are especially concerned with the analysis of parameter uncertainty, and a comparison of measured and modelled H_2O and CO_2 fluxes, including soil moisture dynamics. Finally, the Section on Discussion and Conclusions summarizes the most important conclusions of our study, and recommends additional developments to the concept of VOM to further improve the parameterization and predictive capability of ecohydrological models.

VEGETATION OPTIMALITY MODEL

The coupled water balance, ecophysiological gas exchange, and photosynthesis model presented herein is based on the VOM originally developed by Schymanski (2007) and Schymanski *et al.* (2007) but adapted to include a multi-layer canopy and dynamically varying throughfall fraction. This extended VOM_{mlsc} appears schematically in Figure 1. The original VOM code of Schymanski (2007) and Schymanski *et al.* (2007) assumes a single big-leaf description of the canopy and understorey. This formulation is somewhat appropriate at low LAI, but too simplistic to accurately characterize vegetation properties and dynamics at high LAI (Acock *et al.*, 1978). VOM_{mlsc} therefore uses a multi-layer representation of the canopy to more closely represent the functioning of dense, layered vegetation structures. Moreover, multiple soil horizons are used within VOM_{mlsc} to better represent vertical soil moisture dynamics within the rooting zone. This soil layering improves the description of root moisture uptake, which is of utmost importance in the modelling of transpiration and CO_2 uptake, two main fluxes considered in our detailed evaluation of VOM_{mlsc}. A list of variables and parameters used in VOM_{mlsc} is given in Table I. Rainfall interception is explicitly modelled in VOM_{mlsc} with throughfall made dependent on LAI and gap fraction. This will be discussed in the Section on Above-Ground Processes.

Table II summarizes the VOM_{mlsc} parameters that are subject to calibration, and lists their respective lower and upper bounds as used with the DREAM stochastic optimization algorithm. These parameters include (1) the number of horizontal leaf layers, m (−), in the canopy, (2) the patchiness fraction of the total canopy cover, MA (−), and (3) the maximum rooting depth, y_r (m). These three parameters define static vegetation properties. In addition to these time-invariant vegetation properties, we also selected three parameters that reflect short-term vegetation adaptations, including (4) the initial photosynthetic transport capacity at the top of the canopy, $J_{max,t=0}$ (mol m^{-2} s^{-1}), at $t = 0$, and (5 + 6) two unitless

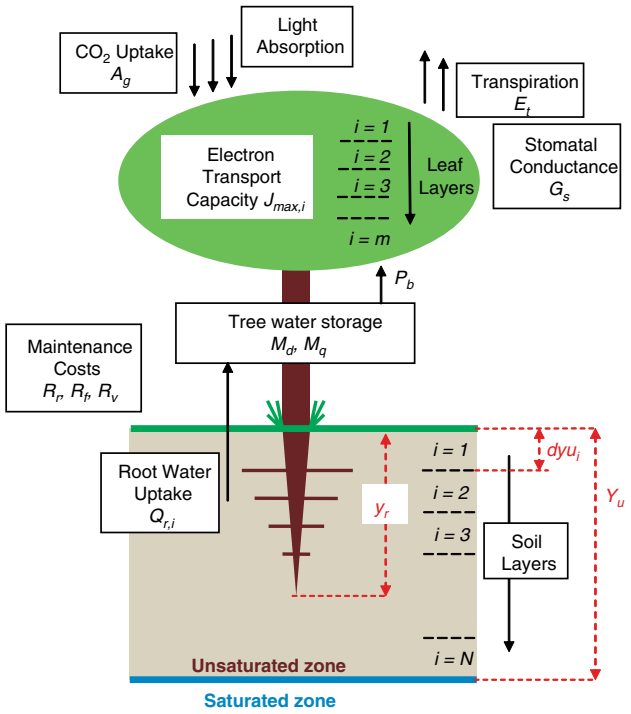

Figure 1. Overview of the multi-layer soil and canopy vegetation optimality model, VOM_{mlsc}, developed herein. This model merges the strengths of a physiological model of light absorption, CO_2 uptake, and plant transpiration, with a one-dimensional Richards' based model of the vadose zone to calculate soil moisture uptake by plant roots, and impose soil moisture constraints on water use. Root water uptake is linked directly to a tree water storage model, which enables hydraulic redistribution. The tissue balance pressure, P_b (bar), depends on the total mass of dry matter (M_d, kg m^{-2}) and the potential water stored in plants (M_q, kg m^{-2}).

DOI: 10.1002/eco

Table I. Parameters and variables used in VOM_{mlsc} and their respective units.

A	Conversion factor translating CO_2 diffusion to H_2O transport	1·6 (−)
A_g	CO_2 uptake rate	mol m^{-2}·s^{-1}
C_a	Mol fraction of atmospheric CO_2	380×10^{-6} mol mol^{-1}
ce	Constant of the relationship between λ and soil water	—
crv	Proportionality constant of carbon costs for water transport	$1{\cdot}2 \times 10^{-6}$ mol m^{-3} s^{-1}
*c*Rr	Root respiration rate per volume fine roots	0·0017 mol m^{-3} s^{-1}
d_{yui}	Thickness of soil layer *i*	0·1 m
D_v	Molar atmospheric vapour deficit	mol mol^{-1}
E_0	Open water evaporation	m s^{-1}
E_s	Soil evaporation	m s^{-1}
E_t	Transpiration	mol m^{-2} s^{-1} (m y^{-1})
G_s	Stomatal conductance	mol m^{-2} s^{-1}
h_i	Matrix suction head in layer *i*	m
$h_{r,i}$	Root suction head in layer *i*	m
I_a	Photosynthically active irradiance (= 51% of I_g)	mol quanta m^{-2}.s^{-1}
I_{cap}	Interception capacity per l	m
I_g	Global irradiance	W m^{-2}
irp	Deepest soil layer accessed by plant roots	—
JA	Photosynthetic electron transport rate per total ground area	mol m^{-2} s^{-1}
$J_{max\,25,i}$	Photosynthetic electron transport capacity at 25 °C	mol m^{-2} s^{-1}
$J_{max\,25,0}$	Maximum photosynthetic electron transport capacity	mol m^{-2} s^{-1}
$\boldsymbol{J_{max,t=0}}$	The initial $J_{max\,25,0}$ at $t = 0$	mol m^{-2} s^{-1}
k	Light extinction coefficient down the canopy	0·5 (−)
$K_{unsat,i}$	Unsaturated soil hydraulic conductivity of later *i*	m s^{-1}
L_i	Cumulative LAI from the top of the canopy	m^2 m^{-2}
L_A	Leaf area of each foliage layer	0·2 m^2
LAI	LAI (= MA $\times m \times L_A$)	m^2 m^{-2}
m	Number of horizontal foliage layers in the canopy	—
MA	Fraction of catchment area covered by vegetation	—
me	Constant of the relationship between λ and soil water	—
M_q	Mass of vegetation water storage	kg m^{-2}
M_{qx}	Maximum vegetation water storage capacity (= M_d)	kg m^{-2}
N	Number of soil layers in the unsaturated zone	—
NCP	Net carbon profit	mol m^{-2}
P	Precipitation rate	m s^{-1}
P_b	Tissue balance pressure	Bar
P_i	Indirect throughfall	m s^{-1}
$Q_{r,i}$	Root water uptake per layer *i*	m s^{-1}
R_{ft}	Carbon cost related to the maintenance of foliage	mol m^{-2} s^{-1}
R_l	Leaf respiration per unit ground area	mol m^{-2} s^{-1}
R_r	Root respiration rate per unit ground area	mol m^{-2} s^{-1}
r_r	Mean radius of fine roots	0·0003 m
R_v	Carbon costs related to water transport tissues	mol m^{-2} s^{-1}
R_w	Woody respiration	mol m^{-2} s^{-1}
$R_{w,25}$	R_w at 25 °C	mol m^{-2} s^{-1}
$SAdr_i$	Root surface area density per unit soil volume	m^2 m^{-2}
t_d	Dry days after a rain event	d
T_w	Temperature of the wood	°C
T_r	Reference temperature	°C
W_u	Unsaturated surface area fraction	—
$\boldsymbol{y_r}$	Maximum rooting depth	m
λ	Slope of the gas exchange curve	mol mol^{-1}
Γ	CO_2 compensation point in the absence of respiration	mol mol^{-1}
Ω_r	Root resistivity to water uptake, constant across all layers	s
$\Omega_{s,i}$	Resistivity of water flow towards the roots in the soil	s

The addition of the subscript *i* indicates, unless stated differently, reference to a specific soil layer. The six VOM_{mlsc} model parameters that are subject to calibration in this study are highlighted in **bold**.

empirical parameters, *ce* (−), and *me* (−) that define the relationship between soil water pressure head and the ratio of transpiration and assimilation. Jointly, these six parameters represent the most important vegetation properties of VOM_{mlsc}. The next section discusses the VOM_{mlsc} model in more detail.

Vegetation optimality model

The combined soil water dynamics, ecophysiological gas exchange, and photosynthesis VOM developed herein are based on a few assumptions that not only simplify the analysis but also speed up the calculations. Irradiance is considered to be the main limiting factor for

DOI: 10.1002/eco

Table II. Summary statistics of the DREAM-derived parameter distribution by optimality against NCP (mol·m^{-2}) using the 1995 data set from the Speuldersbos.

			DREAM				DREAM	SCE-UA
	Initial range		Calibration results				MAX_{NCP}	
	Minimum	Maximum	Minimum	Maximum	Mean	CV		
MA	0·20	1·00	0·96	1·00	0·99	0·6	1·00	1·00
y_r	0·50	5·00	0·50	0·72	0·54	7·1	0·51	0·50
ce	1·00	5·00	2·63	4·69	3·55	9·5	3·31	3·13
Me	−3·00	1·00	−1·26	0·16	−0·45	47·2	−0·28	−0·21
M	2	60	8	17	11	11·7	11	11
$J_{max,t=0}$	10·0	450	86	447	247	20·5	222	219
NCP	—	—	117·8	129·1	125·6	1·5	129·1	128·9

We list the prior ranges, mean, minimum, maximum, and CV of the individual parameters. We also report the point of the joint chains that exhibits the highest value of NCP. This solution is referred to as MAX_{NCP}. To benchmark the results of DREAM we include the MAX_{NCP} values of the parameters separately derived with the SCE-UA global optimization algorithm. The parameters are MA (−) patchiness of vegetation, y_r (m) rooting depth, *m* (−) number of horizontal canopy layers, *ce* + *me* (−) empirical parameters defining water use efficiency, and $J_{max,t=0}$ (μmol·m^{-2}·s^{-1}) maximum initial value of the photosynthetic transport capacity at the top of canopy. The listed DREAM-statistics were derived from the last 5000 solutions stored in the various Markov chains.

photosynthesis, and biochemical carboxylation capacity is consequently ignored (Farquhar and von Caemmerer, 1982). Costs of nutrient uptake are also neglected, as this particular process is poorly understood and hence difficult to quantify. For more details see Schymanski (2007) and Schymanski *et al*. (2007, 2009).

Above-ground processes. A leaf can achieve a maximum CO_2 uptake for any given amount of total water available for transpiration if it adjusts its stomatal conductance (G_s in mol m^{-2} s^{-1}) in such a way that the marginal cost of assimilation (λ in mol mol^{-1}) is maintained at a constant value (Cowan and Farquhar, 1977):

$$\lambda = \frac{\partial E_t}{\partial A_g} \tag{1}$$

where E_t (mol m^{-2} s^{-1}) denotes the actual transpiration and A_g (mol m^{-2} s^{-1}) is the rate of CO_2 assimilation. To optimize G_s, the value of λ is fixed and used to compute the instantaneous E_t, given current environmental conditions of vapour pressure deficit (VPD), atmospheric CO_2 concentration (C_a in mol mol^{-1}), instantaneous electron transport rates (JA in mol m^{-2} s^{-1}), and leaf respiration (R_l in mol m^{-2} s^{-1}). Once E_t is known, the value of G_s can be computed as follows:

$$G_s = \frac{E_t}{aD_v} \tag{2}$$

where *a* (−) is a unitless constant of 1·6 to convert CO_2 diffusion across the stomata to H_2O transport, and D_v signifies the water vapour deficit (mol mol^{-1}). Finally, CO_2 uptake can be derived from the actual value of G_s:

$$A_g = \frac{1}{8}[4C_aG_s + 8\Gamma G_s + JA - 4R_l] - \frac{1}{8}\sqrt{\begin{matrix}(-4C_aG_s + 8\Gamma G_s + JA - 4R_l)^2 \\ +16G_s(8C_aG_s + JA + 8R_l)\Gamma\end{matrix}} \tag{3}$$

in which Γ (mol mol^{-1}) defines the temperature dependent CO_2 compensation point. The value of λ is dependent on the available soil moisture within the rooting zone:

$$\lambda = 10^{ce}\left(\sum_{i=1}^{irp} h_i\right)^{me} \tag{4}$$

where h_i (m) denotes the soil water pressure head of soil layer i; $i = 1, \ldots, N$, irp (−) is the deepest soil layer from which the roots are taking up water, and *ce* (−) and *me* (−) are unitless empirical parameters that define the functional shape of the relationship between λ and h. As discussed in the Section on Vegetation Optimality Model, the variables *ce* and *me* are considered to be unknown parameters whose values are subject to calibration.

As part of our study, we extend the original VOM formulation to include a multi-layer representation of the canopy. This model is hereafter referred to as VOM_{mlsc} and is especially designed to provide a better description of the field site. In VOM_{mlsc}, the canopy is subdivided into different horizontal layers of foliage, each with an equal leaf area (L_A) of 0·2 m^2. The temperature dependence of the photosynthetic electron transport capacity ($J_{max,i}$, mol m^{-2} s^{-1}), is calculated empirically per leaf layer $i = 1, \ldots, m$ following Medlyn *et al*. (2002). This requires knowledge of the electron transport capacity at 25 °C ($J_{max\,25,i}$, mol m^{-2} s^{-1}) in each of the *m* canopy layers. Various contributions to the ecological literature have shown that the allocation of $J_{max,i}$ within the canopy follows closely the integrated light availability (Niinemets *et al*., 1999; Misson *et al*., 2006). We therefore calculate $J_{max\,25,i}$ using an exponential decay function of light down the canopy (Thornley, 2002):

$$J_{max\,25,i} = J_{max\,25,0}e^{-kL_i} \tag{5}$$

where $J_{max\,25,0}$ (mol m^{-2} s^{-1}) is the maximum possible value of $J_{max\,25}$ (mol m^{-2} s^{-1}) for fully exposed leaves at

DOI: 10.1002/eco

the top of the canopy, k (−) is a unitless extinction coefficient (Duursma *et al*., 2003), and L_i (m^2 m^{-2}) represents the cumulative LAI for each individual canopy layer, measured from the upper canopy surface. In all our calculations, we assume that $k = 0{\cdot}5$ and allow $J_{\max 25,0}$ to vary dynamically from day to day in response to changing light conditions. A maximum daily change in $J_{\max 25,0}$ of 1% was deemed appropriate. To initialize $J_{\max 25,0}$ we use a calibration parameter $J_{\max,t=0}$ representing the $J_{\max 25,0}$ at $t = 0$.

Interception of rainfall water by the canopy constitutes an important component of the water balance and exerts a strong influence on the three-dimensional distribution and availability of soil moisture. Canopy cover and LAI determine throughfall dynamics, but these controlling factors are not considered in the original VOM model of Schymanski (2007) and Schymanski *et al*. (2007). To better represent throughfall, we differentiate between direct (P_d; m s^{-1}) and indirect (P_i; m s^{-1}) throughfall. Indirect throughfall, P_i, is the amount of water that does not evaporate within a given time step Δt, and is limited by the interception capacity, I_{cap} (m^3 m^{-2} leaf):

$$P_i = \text{MA} \times P - \min(E_0, \text{LAI} \times I_{\text{cap}}/\Delta t) \qquad (6)$$

where P (m s^{-1}) is gross precipitation, MA (−) is the throughfall fraction (as defined previously), E_0 (m s^{-1}) represents the open water evaporation, and LAI (m^2 m^{-2}) is the leaf area index. On the basis of the work presented in Brolsma and Bierkens (2007), we set $I_{\text{cap}} = 5 \times 10^{-4}$ m. The sum of P_i and P_d, defined as (1 − MA) P, is the total amount of throughfall.

Below-ground processes. To calculate soil moisture flow and root uptake, we discretize the soil profile into N different horizontal layers with equal thickness. The exceptions are the surface layer (dyu_1) whose lower boundary is always fixed at 10 cm depth, and the bottom layer whose thickness varies with the dynamically changing water table. Movement of water between individual soil layers is calculated from numerical solution of Richards' equation using the Mualem van Genuchten (MVG) (Mualem, 1976; van Genuchten, 1980) constitutive relationships of pressure head, soil water content, and hydraulic conductivity. Root water uptake ($Q_{r,i}$ in m s^{-1}) is calculated in each discretized soil layer from the respective difference between matrix and root water pressure head, $h_{r,i}$ (m):

$$Q_{\text{r},i} = SAr_{\text{i}} \frac{h_{\text{r},i} - h_i}{\Omega_{\text{r}} + \Omega_{\text{s},i}} \qquad (7)$$

where Ω_{r} (s) denotes the resistivity of the roots to water uptake, SAr_i (m^2 m^{-2}) is the area of the root surface for a given soil area, and $\Omega_{s,i}$ (s) defines the resistivity of water flow towards the soil roots. In VOM, $\Omega_{s,i}$ is computed for each individual soil layer, $i = 1, \ldots, N$ as follows:

$$\Omega_{\text{s},i} = \frac{1}{K_{\text{unsat},i}} \sqrt{\frac{\pi \times r_r}{2\text{SA}r_i}} \qquad (8)$$

in which r_{r} (m) represents the root radius, and $K_{\text{unsat},i}$ (m s^{-1}) is the unsaturated soil hydraulic conductivity, which is a function of saturation degree.

For the below-ground processes, we have included different soil horizons. In all calculations reported herein, we use a single value of Ω_{r} for all soil layers, and fix the MVG water retention and unsaturated soil hydraulic conductivity functions using inversion results from multi-step outflow and evaporation experiments on small soil cores.

The root water uptake model defined in Equation (7) requires accurate estimates of the root surface area and the resistivity of the soil and root against water flow. In the absence of compelling prior information about these root and soil properties, we consider the following optimality approach in VOM_{mlsc}. First, the value of *SAdr* is adapted on a daily basis for each individual soil layer to meet the transpiration demands during the previous day. Depending on two variables, SAdr_i was optimized based on firstly the ability of the roots to meet the tree's water demand during the previous day, calculated using the minimum water storage achieved the previous day (M_{qmin} in kg m^{-2}) and known as the 'coefficient of change' (K_{r}). Secondly, the relative effectiveness of the roots in each soil layer over the previous 24 h ($K_{\text{reff},i}$), in relation to the roots in other soil layers, was taken into account. This short-term adaptation is considered appropriate to deal optimally with changing environmental conditions. Then, the maximum rooting depth, y_{r}, is treated as an optimization parameter, and assumed to be constant over the simulation period.

Soil evaporation, E_s (m s^{-1}), was computed using the approach of Black *et al*. (1969):

$$E_{\text{s}}(t) = red \times \frac{E_0}{\Delta t}(1 - \text{MA}) \left(\sqrt{t_{\text{d}} + 1} - \sqrt{t_{\text{d}}} \right) \qquad (9)$$

where *red* (−) is a unitless reduction parameter. On the basis of the work presented by Dekker *et al*. (2001) the value of *red* is derived from $\min(0{,}1 - h_1/60)$, where h_1 (m) denotes the pressure head of the top layer and t_{d} (day) signifies the number of dry days after a rain event.

Interaction of above- and below-ground. In real-world vegetation, processes of photosynthesis, stomatal conductance, and soil moisture dynamics are coupled to control transpiration. To mimic this coupling, VOM_{mlsc} implements an explicit feedback between soil water availability and transpiration. The first control considers root-induced stomatal closure. If the actual water storage (M_{q}, kg m^{-2}) of the Douglas-fir drops below 90% of the potential water storage (M_{qx}, kg m^{-2}), VOM_{mlsc} imposes the constraint that transpiration cannot exceed root water uptake. This avoids cavitation. The second control involves dynamic adaptation of the stomatal conductance of the leaves. This is dictated by the variable λ, whose value in turn depends directly on soil moisture availability. This is quantified in Equation (4).

DOI: 10.1002/eco

Optimality hypothesis and criteria used

As argued in the Section on Introduction, different hypotheses can be formulated to help analyse and understand plant functioning. In keeping with previous studies (Schymanski, 2007; Schymanski *et al*., 2007, 2008), we assume the principle of vegetation optimality, and hypothesize that the vegetation adapts itself dynamically in such a way that it maximizes NCP over the considered simulation period. In the following development, the symbol t denotes time, whereas t_{start} and t_{end} refer to the start (1 January) and end time (31 December) of the VOM_{mlsc} simulation.

In the remainder of this article, NCP is defined as the difference between photosynthetic CO_2 uptake (A_g) (defined in the previous section), and the carbon costs of the leaves (R_{ft}, mol m^{-2} s^{-1}), the vascular system (R_v, mol m^{-2} s^{-1}), and the roots (R_r, mol m^{-2} s^{-1}):

$$\text{NCP} = \sum_{t_{\text{start}}}^{t_{\text{end}}} [A_g(t) - R_{\text{ft}}(t) - R_v(t) - R_r(t)]\Delta t \qquad (10)$$

Foliage turnover costs (R_{ft}) for Douglas-fir are estimated from GLOPNET (Wright *et al*., 2004). Following Schymanski (2007) and Schymanski *et al*. (2007), construction costs were assumed to be 2 g CO_2 per gram leaf dry matter (Givnish, 2002), which allows the costs of foliage turnover to be directly determined from LAI (m^2 m^{-2}):

$$R_{\text{ft}} = 4 \times 10^{-8} \times \text{LAI} \qquad (11)$$

The parameters R_v and R_r that are associated with the maintenance costs of the vascular and rooting systems are calculated from the proportionality constants given in Schymanski (2007) and Schymanski *et al*. (2007). Root respiration, $R_{r,i}$, $i = 1, \ldots, N$ is computed for each individual soil layer using:

$$R_{r,i} = cRr \left(\frac{1}{2} r_r \times SAdr_i \times dyu_i \times W_u \right) \qquad (12)$$

where cRr (mol m^{-3} s^{-1}) is a root proportionality constant, r_r (m) signifies the mean radius of the fine roots, SAdr_i (m^2 m^{-3}) represents the density of the surface area of the roots in each of the N different soil layers, dyu_i (m) is the thickness of soil layer i, and W_u denotes a unitless unsaturated surface area fraction. On the basis of the work presented in Schymanski *et al*. (2009), we use values of $c\text{Rr} = 1{\cdot}7 \times 10^{-3}$ mol m^{-3} s^{-1}, and $r_r = 3{\cdot}0 \times 10^{-4}$ m. Finally, the maintenance costs of the vascular system (R_v) are derived from the parameters MA and y_r:

$$R_v = crv \times \text{MA} \times y_r \qquad (13)$$

where crv (mol m^{-3} s^{-1}) is a proportionality constant that is assumed to be $1{\cdot}2 \times 10^{-6}$ mol m^{-3} s^{-1} (Schymanski *et al*., 2009).

STUDY SITE AND MEASUREMENTS

The VOM_{mlsc} model is tested and evaluated using atmospheric forcing data and soil and vegetation properties from a Douglas-fir forest in The Netherlands. This forest, also called the Speuldersbos, was planted in 1962 and data was collected at our experimental field site of about 2·5 ha in close proximity of the village of Garderen (longitude 5·73° and latitude 52·3°). The tree density of the Douglas-fir stand equals about 780 trees ha^{-1}, with a mean tree height of ∼21·6 m. There is no understorey present at the field site, and the projected LAI ranges between 7·8 and 10·5 m^2 m^{-2}. The soil is a well-drained Haplic Podzol consisting of fluviatile deposits with textures ranging from fine sand to sandy loam. A detailed soil survey has demonstrated that the vadose zone consists primarily of three distinctly different soil types. We use this knowledge to set up a three-layer Richards' based model of the unsaturated zone. Note that this implantation of VOM_{mlsc} deviates somewhat from the original code of Schymanski (2007) and Schymanski *et al*. (2007) which uses a single horizon soil layer only. The groundwater table is nearly stationary at about 40 m below the soil surface, and the 30-year mean rainfall rate equals ∼834 mm y^{-1}.

Atmospheric forcing data used as input to VOM_{mlsc} were measured in a 36 m tower at the experimental site by the Royal Meteorological Institute of The Netherlands (KNMI). These measurements include half-hourly observations of temperature (T_a, °K), global irradiance (I_g, W m^{-2}), rainfall (P, m s^{-1}), and VPD (mbar). In addition, photosynthetically active radiation (PAR, I_a) was assumed to be 51% of the global radiation, which is a typical value for this particular area (Britton and Dodd, 1976).

The focus of this article is on the year 1995. Initial soil hydraulic heads, relative root distribution, and soil properties are taken from Tiktak and Bouten (1994) and Van Wijk *et al*. (2001). The top metre of the soil contains about 75% of the roots, whereas the remaining fraction of roots is found at a depth between 1·0 and 2·5 m (Tiktak and Bouten, 1994). Such root profile is common for temperate coniferous forests (Jackson *et al*., 1996), and we therefore adopt this root distribution in VOM_{mlsc} for all calculations reported herein. The top 40% of the rooting zone was assumed to contain 75% of the roots, whereas the remaining fraction of roots (0·25) is stored in the bottom 60% of the rooting zone, i.e. at depths between $0{\cdot}4y_r$ and $1{\cdot}0y_r$, below the soil surface. Hence, the maximum rooting depth (y_r) acts as a scaling parameter in this approach, and we determine its value by calibration using DREAM. Soil respiration rates were calculated using a relatively simple multiplicative function (Freijer *et al*., 1997; Van Wijk *et al*., 2001). Woody respiration (R_w) was calculated by Schymanski (2007) and Schymanski *et al*. (2007)

$$R_w = R_{w,25} \times Q_{10}^{(Tw-Tr)/10} \qquad (14)$$

where $R_{w,25}$ is the R_w at reference temp (T_r, 25 °C) and T_w (°C) denotes the temperature of the wood. In this study, $R_{w,25}$ was taken to be 0·85 10^{-6} molCO_2 m^{-2} s^{-1} to match observed fluxes of woody respiration at the same

DOI: 10.1002/eco

experimental site (Van Wijk *et al*., 2001). Finally, the ratio between diffuse and direct sunlight was estimated from the relationship between global and top-of-the-atmosphere irradiance (Spitters *et al*., 1986; Schymanski, 2007; Schymanski *et al*., 2007).

To evaluate the usefulness of the NCP optimality hypothesis considered herein, we compared the VOM_{mlsc} predictions of transpiration, CO_2 uptake, and root-zone soil moisture with respective measurements of these different quantities. Half-hourly observations of evapotranspiration and CO_2 fluxes were made during the summer of 1995 with the eddy correlation measurement technique. Flux measurements during rainfall events or with a wet canopy were excluded from the final data set, resulting in a total of 43 days of half-hourly measurements of H_2O and CO_2 flux observations. Soil moisture measurements were made using five different vertically installed TDR probes between depths of 5 and 35 cm.

OPTIMIZATION STRATEGY OF VOM_{MLSC}

Now our multi-layer soil and canopy model VOM_{mlsc} has been mathematically formulated, the task that remains is to estimate the unknown values of the six model parameters. These parameters are listed in Table II, including their upper and lower bounds. These ranges appear rather large, and have been derived from our knowledge of the actual vegetation and measurements of eddy correlation, meteorological data, and soil moisture. The selection of the bounds should not affect the final optimized parameter distribution, but only determines the efficiency of the stochastic search. The larger the prior ranges the more function evaluations DREAM will need to search the parameter space and converge to a limiting distribution.

We adopt the principle of vegetation optimality and consider NCP to be our main calibration target. Evaluation is based on the same 1-year data set. In principle, this maximization can be done manually by trial and error using repeated VOM_{mlsc} runs. Unfortunately, this approach is rather inefficient and time consuming, especially with increasing number of parameters to be estimated. Previous work by Schymanski (2007) and Schymanski *et al*. (2007) have therefore used the SCE-UA global optimization algorithm for automatic optimization of the parameters in the original big-leaf VOM. The SCE-UA method merges the strengths of controlled random search, downhill Simplex evolution, and complex shuffling to efficiently search the parameter space for the global optimum. In this article, we have used the SCE-UA algorithm to optimize the parameters of VOM_{mlsc}.

For highly parameterized models of environmental systems it still remains difficult, if not impossible, to find a single 'best' point in the parameter space whose performance measure differs significantly from other feasible parameter combinations. Vrugt *et al*. (2003b) have therefore modified the SCE-UA method to facilitate converging to a distribution of behavioural parameter values, rather than a single 'best' point. This method, entitled the shuffled complex evolution metropolis (SCEM-UA) algorithm, is an adaptive MCMC sampling scheme that runs multiple Markov chains simultaneously in parallel for posterior exploration. These chains learn from each other through the use of a common population of external points, which collectively contain the information about the progress of the search. After a burn-in period, the states of the individual chains are independent, so that convergence of an SCEM-UA run can be monitored with the $\hat{R}$ diagnostic of Gelman and Rubin (1992).

In this study, we use the DREAM algorithm recently presented by Vrugt *et al*. (2008, 2009a,b) to explore the VOM_{mlsc} parameter space for high NCP values. The DREAM sampling scheme is an adaptation of the SCEM-UA global optimization algorithm, but has the advantage of maintaining detailed balance and ergodicity, while showing good efficiency on complex, highly nonlinear, and multimodal target distributions (Vrugt *et al*., 2009a). A detailed description of the algorithm appears in Vrugt *et al*. (2008, 2009a) and is beyond the scope of this article.

We run the DREAM algorithm with standard settings of the algorithmic variables using the parameter bounds listed in Table II with 20 different Markov chains and 50 000 VOM_{mlsc} evaluations. Our experience with other parameter estimation problems of similar dimension suggests that these settings are appropriate. The only difficulty that remains is what likelihood function to use in DREAM to efficiently explore the parameter space for high NCP values. The following likelihood function, $L(\theta|\mathbf{Y})$ provides a simple exponential mapping from NCP to probability space

$$L(\theta|Y) = \exp(\mathrm{NCP}) \tag{15}$$

where θ represents the vector of unknown model parameters, and $\mathbf{Y}$ contains all forcing and other input data, needed to run VOM_{mlsc}. This monotonically increasing function works well in practice and ensures that DREAM will converge towards solutions with the highest NCP values. Better solutions with higher NCP values receive a higher likelihood and are therefore preferentially sampled. In the absence of compelling information about the values of the model parameters, we utilize a uniform prior distribution of $p(\theta)$ with ranges specified in Table II.

The results reported herein are derived from the last 5000 parameter combinations stored in the individual chains generated with DREAM. These parameter values correspond to the stationary distribution of $p(\theta|\mathbf{Y})$, and define parameter and predictive uncertainty. Note that random or stratified sampling could also have been used to explore the six-dimensional parameter spaces of VOM_{mlsc} for solutions that give high NCP values. Yet, this approach is very inefficient, and can result in an algorithm that, even after billions of model evaluations, may only have generated a handful of good solutions. The main advantage of DREAM is thus sampling efficiency.

DOI: 10.1002/eco

RESULTS

Distribution of parameter values

Table II lists values of the DREAM-derived posterior mean, minimum, maximum, and coefficient of variation (CV) of the six VOM_{mlsc} parameters by optimality against NCP. For completeness, we also report the point of the DREAM sample that exhibits the highest NCP. This solution is hereafter referred to as MAX_{NCP}, and compared to the solution separately derived with the SCE-UA algorithm. Most of the VOM_{mlsc} parameters are poorly identified by optimality against NCP with posterior ranges that occupy a significant portion of the feasible parameter space. The exceptions are the patchiness of the vegetation (MA), and maximum rooting depth (y_r) whose solutions span only a relatively small part of the prior distribution. Of course, the ranges derived with DREAM are contingent upon the choice of the likelihood function used to translate NCP into a probability density. Yet, irrespective of this conversion function, considerable changes in most of the parameters are required to noticeably change NCP in the vicinity of its optimum value.

The MAX_{NCP} values of the parameters appear well within the ranges, with the exception of MA and y_r whose optimized values appear at the bound. These bounds enforce the parameters to remain physically realistic, and are required in the presence of structural inadequacies in VOM_{mlsc}. The MAX_{NCP} solution of DREAM exhibits a value of NCP of about 129·1 (mol m^{-2}) which is somewhat larger than its counterpart of 128·9 (mol m^{-2}) separately derived with the SCE-UA global optimization algorithm. This finding inspires confidence that DREAM has successfully located the area of maximum NCP values. Yet, both methods differ somewhat in their MAX_{NCP} estimates of *ce* and *me*. The ability of DREAM to maintain diversity during the search enables jumps out of small pits which frequently appear in the vicinity of the global minimum.

Figure 2 presents histograms of the DREAM-derived marginal distributions of the VOM_{mlsc} parameters (a) MA (−) fraction of vegetation cover, (b) y_r (m) maximum rooting depth, (c) *m* (−) number of horizontal canopy layers, (d + e) *ce* (−) + *me* (−): empirical parameters defining water use efficiency, and (f) $J_{max,t=0}$ (μmol m^{-2} s^{-1}) maximum photosynthetic transport capacity at the top of the canopy at $t = 0$. These histograms were derived by optimality of VOM_{mlsc} against NCP using the last 250 parameter combinations stored in each of the 20 different Markov chains. This results in a sample of 5000 points. The top three panels (Figure 2a–c) depict histograms for the static vegetation properties, whereas the bottom three graphs

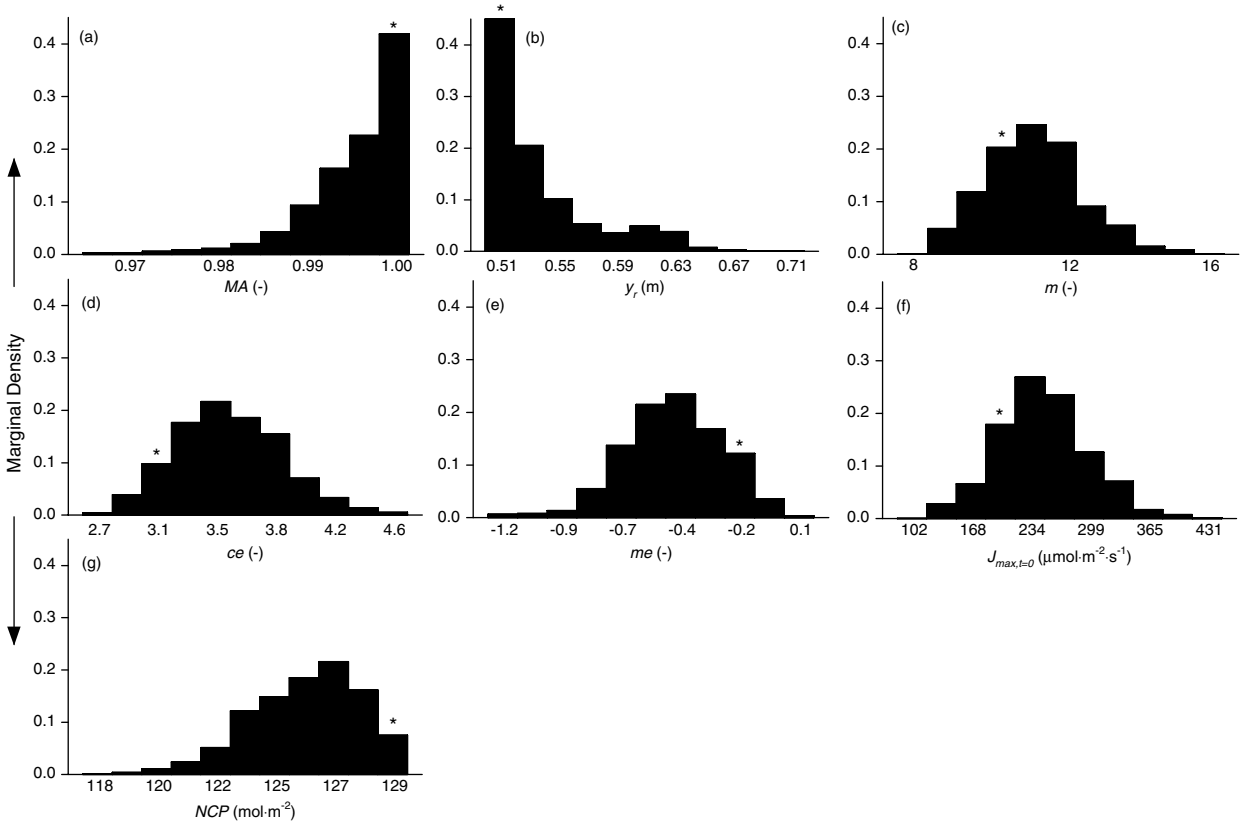

Figure 2. Optimality of NCP: DREAM-derived marginal distributions of the six different VOM_{mlsc} parameters using the 1995 data set from the Speuldersbos in The Netherlands, (a) MA (−) fraction of vegetation cover, (b) y_r (m) maximum rooting depth, (c) *m* (−) number of horizontal canopy layers, (d + e) *ce* (−) + *me* (−): empirical parameters defining the slope, λ, of the gas exchange curve, (f) $J_{max,t=0}$ (μmol.m^{-2}·s^{-1}) maximum initial value of the photosynthetic transport capacity at top of the canopy, and (g) marginal distribution of DREAM-inferred NCP values. The SCE-UA-derived parameter values that maximize NCP are separately indicated in each plot with the symbol '*'.

DOI: 10.1002/eco

(Figure 2d–f) illustrate the results for the three remaining VOM_{mlsc} parameters that define dynamic vegetation properties. A histogram of associated NCP values is also included (Figure 2g). For completeness, the SCE-UA-derived parameter values that maximize NCP are separately indicated in each plot with the symbol '*'.

The results presented in this figure highlight several interesting observations. First, for most parameters, the mode of the DREAM sample of 5000 solutions matches closely with the SCE-UA-derived solution. This inspires confidence that DREAM has converged to the appropriate limiting distribution. The mode of the histograms of *ce* and *me* deviate somewhat from their SCE-UA-derived counterparts. This discrepancy is explained by parameter correlation and insensitivity. Second, the histograms display significant parameter variation. This suggests that many different plant species can co-exist that exhibit very similar (optimal) NCP values. The scale and orientation of the DREAM-inferred parameter distributions provide important diagnostic information about VOM_{mlsc}, and help understand and analyse vegetation behaviour and dynamics. Third, most of the histograms of the VOM_{mlsc} parameters depart from a normal distribution. The hypothesis of vegetation optimality causes y_r to converge to its lower bound (Figure 2b), whereas MA (Figure 2a) takes on values at its upper bound. The presence of such bounds causes the marginal distributions of MA and y_r to be significantly skewed. On the contrary, the remaining vegetation properties depicted in the other panels (Figure 2c–f), exhibit a somewhat log-normal distribution with negative (Figure 2e: *me*) or positive (Figure 2c: *m*, Figure 2d: *ce* and Figure 2f: $J_{max,t=0}$) skew. The results presented in Figure 2 illustrate that the value of NCP can be further increased if we relax the upper and lower bound of MA and y_r, respectively. Unfortunately, this is physically impossible (MA cannot be larger than 1·0), or allows for vegetation characteristics that are deemed inappropriate for the Douglas-fir stand under consideration. For example, a detailed investigation of the three-dimensional rooting system of a Douglas-fir tree in the Speuldersbos has shown that the minimum rooting depth, y_r, at the experimental site is at least 50 cm. This value is therefore used as lower bound, and ensures that y_r remains physically realistic. Finally, the DREAM-derived marginal distributions generally encompass a significant portion of the prior parameter ranges. This explains the relative high CVs for most of the parameters (Table II), particularly for $J_{max,t=0}$, and the parameters *ce* and *me* that define the functional shape of the water use relationship between λ and soil water pressure head. Altogether, our findings illustrate a significant variation in optimized vegetation properties and characteristics from ecohydrological optimality of NCP. Seemingly, a myriad of vegetation species is possible that results in very similar (optimal) values of NCP.

To determine whether VOM_{mlsc} is of appropriate complexity consider Table III, which lists correlation coefficients between the model parameters of the DREAM sample of solutions. For completeness, we also include estimates of correlation between the model parameters, and VOM_{mlsc} simulated values of NCP, cumulative evapotranspiration (ΣET), cumulative photosynthetic CO_2 uptake (ΣCO_2), and the mean slope of the gas exchange curve ($\overline{\lambda}$), over the 1-year simulation period. To provide further insights into these dependencies, Figure 3 presents two-dimensional scatter plots of selected pairs of parameters and/or different diagnostic variables, including *ce* and *me* (Figure 3a), *ce* and ΣET (Figure 3b), *me* and ΣET (Figure 3c), $\overline{\lambda}$ and ΣET (Figure 3d), ΣCO_2 and NCP (Figure 3e), and ΣCO_2 and ΣET (Figure 3f). Each dot in each graph represents a different solution of the DREAM sample.

Most of the VOM_{mlsc} model parameters exhibit negligible correlation with *r*-values that are smaller than 0·3. This not only provides strong support for the claim that VOM_{mlsc} is of appropriate complexity for the site under consideration but also demonstrates that the principle of NCP optimality has considerable diagnostic power. At least four calibration parameters, defining the most important static and dynamic vegetation properties of VOM_{mlsc}, are identifiable by calibration against NCP. The only two parameters that remain difficult to estimate are *ce* and *me*. The mathematical formulation of Equation (4)

Table III. DREAM-inferred correlation between the six different VOM_{mlsc} parameters, net carbon profit (NCP, mol m^{-2}), the average slope ($\overline{\lambda}$, mol mol^{-1}) between assimilation and evapotranspiration, modelled cumulative CO_2 flux (ΣCO_2, mol m^{-2}), and modelled cumulative transpiration (ΣET, m) using the 1995 data set from the Speuldersbos.

	MA	y_r	*ce*	*me*	*m*	$J_{max,t=0}$	NCP	ΣET	ΣCO_2	$\overline{\lambda}$
MA	1·00									
y_r	0·02	1·00								
ce	−0·02	0·06	1·00							
me	0·02	0·04	**−0·95**	1·00						
m	0·02	0·07	−0·06	0·03	1·00					
$J_{max,t=0}$	0·03	−0·06	−0·03	0·01	−0·21	1·00				
NCP	0·44	−0·57	−0·16	0·19	−0·09	−0·03	1·00			
ΣET	−0·07	0·17	**0·88**	**−0·69**	−0·09	0·05	−0·10	1·00		
ΣCO_2	0·41	0·23	0·25	0·00	0·14	−0·06	0·47	0·54	1·00	
$\overline{\lambda}$	−0·02	0·05	**0·94**	**−0·84**	−0·09	−0·05	−0·20	**0·89**	0·25	1·00

Correlation values (abbreviated as *r* in the main text) that are larger than 0·6 are highlighted in **bold**.

DOI: 10.1002/eco

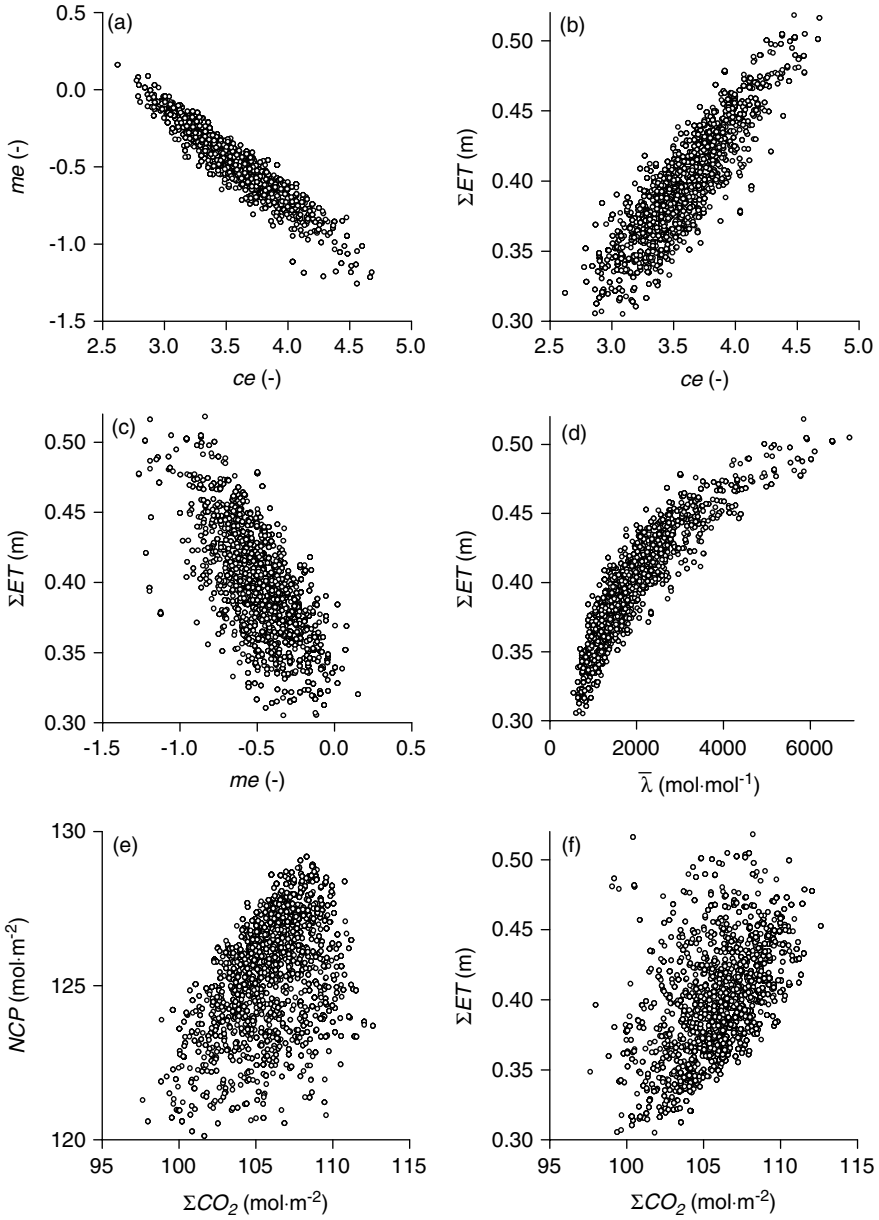

Figure 3. Optimality of NCP: Two-dimensional scatterplots of the DREAM ensemble of dynamic vegetation parameters, cumulative assimilation (ΣCO_2, mol m^{-2}), cumulative transpiration (ΣET, mol m^{-2}), and average slope of the gas exchange curve ($\bar{\lambda}$,mol mol^{-1}) for the 1995 data set from the Speuldersbos. Each dot in each individual graph represents a different solution of the DREAM ensemble, (a) *ce* against *me*, (b) *ce* against ΣET, (c) *me* against ΣET, (d) $\bar{\lambda}$ against ΣET, (e) ΣCO_2 against NCP, and (f) ΣCO_2 against ΣET.

causes these two parameters to be almost perfectly linearly correlated ($r = -0{\cdot}95$) which makes inference of the water use efficiency relationship in VOM_{mlsc} particularly difficult. In the absence of additional field data, future work should therefore simplify this water use relationship using only a single calibration parameter. The relatively strong linear correlation between ce and ΣET (Figure 3b), and me and ΣET (Figure 3c), so evidently present in their respective scatter plots is also determined by Equation (4). This linear correlation causes large variations in cumulative yearly evapotranspiration amounts, suggesting the presence of a wide range of species that is associated with optimal NCP values. Furthermore, the mildly nonlinear (hyperbolic) correlation ($r = 0{\cdot}89$) between $\bar{\lambda}$ and ΣET in Figure 3d is the direct result of Equation (1). Indeed, higher values of λ increase transpiration.

Figure 4a illustrates the time evolution of $J_{max,0}$ at the experimental field site in the Speuldersbos during the calibration year 1995. The dark line represents the DREAM-derived mean ensemble simulation, whereas the dotted lines denote the time evolution of the corresponding standard deviation. The initial value of $J_{max,t=0}$ at the start of simulation (1 January 1995) exhibits considerable variation with values ranging between 200 and 300 μmol m^{-2} s^{-1}, and corresponding CV value of 20·5% (Table II). The dynamic day-to-day adjustment of $J_{max,0}$ causes the sample of DREAM solutions to collapse during the 1995 season. After 365 days the uncertainty has become negligibly small. The marginal distributions

DOI: 10.1002/eco

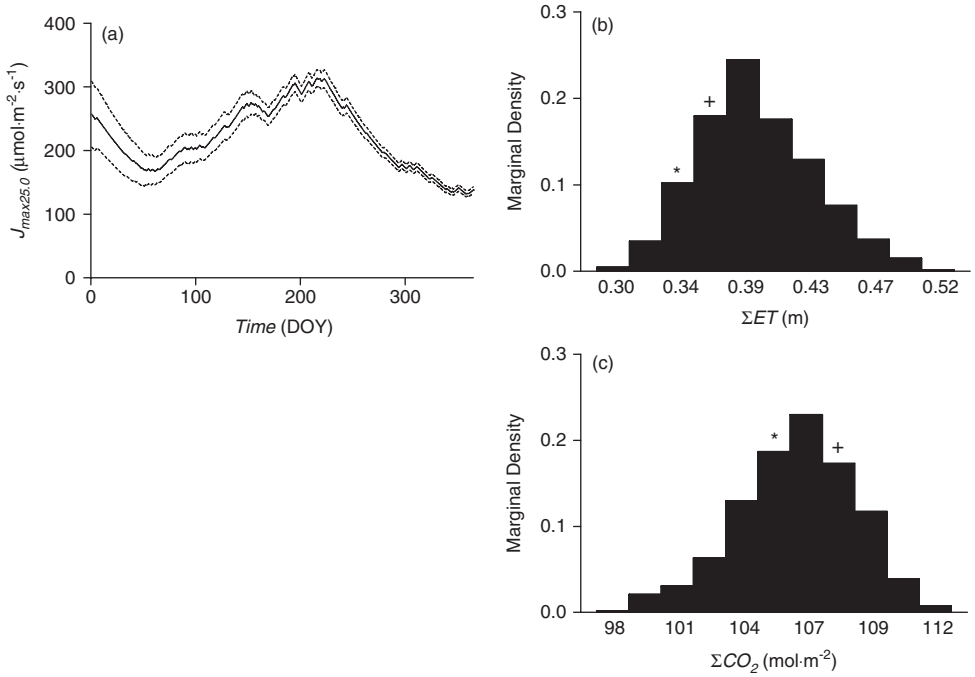

Figure 4. (a) Dynamic evolution of $J_{\max 25,0}$ (µmol m^{-2} s^{-1}) at the Speuldersbos during the year 1995. Dotted lines represent standard deviations that are derived from the DREAM sample of 5000 solutions. (b + c) Marginal distributions of ΣET and ΣCO_2 derived from the ensemble. The SCE-UA and DREAM maximum likelihood are respectively indicated by a '*' and '+'.

of ΣET (Figure 4b) and ΣCO_2 (Figure 4c) show considerable variation, suggesting that many different species exist that result in very similar values of NCP. In particular, the cumulative transpiration, ΣET ranges between 0·30 and 0·52 m, and ΣCO_2 ranges between 98 and 112 mol m^{-2}.

The results presented so far illustrate that there are important advantages to working with a distribution of (optimal) parameter sets rather than a single solution. The ensemble of solutions demonstrates the presence of a significant correlation between *ce* and ΣET ($r = 0{\cdot}88$) and between $\overline{\lambda}$ and ΣET ($r = 0{\cdot}89$) over the 1-year calibration period. The SCE-UA algorithm which is designed to find a single best NCP solution does not convey this information. From the joint and marginal distributions of the structural parameters we further conclude that many different plant species lead to very similar (optimal) values of NCP.

Comparison of measured and modelled VOM $_{\text{mlsc}}$ *predictions*

In this section we compare model simulations of plant transpiration, CO_2 uptake, and root-zone soil moisture dynamics with observations of these respective quantities using eddy correlation and TDR measurements. Figure 5a and b compares daytime measured half-hourly flux observations of CO_2 and ET with their DREAM-derived mean ensemble modelled counterparts for a period of 240 h. The actual modelled CO_2 flux is derived from the half-hourly CO_2 uptake rate (A_g in mol m^{-2} s^{-1}) simulated with VOM_{mlsc} minus soil and woody respiration, and represents the mean of the ensemble of 5000 solutions derived with DREAM. The dotted lines represent the standard deviation of the ensemble. These lines are hardly visible and unfortunately only intelligible at daytime when some differences occur in the flux predictions of the different ensemble members.

Figure 5c compares mean ensemble model predictions of half-hourly CO_2 fluxes against their respective measurements using the eddy correlation measurement technique ($r = 0{\cdot}79$). The predictions of VOM_{mlsc} generally overestimate the actual observed CO_2 fluxes with an overall bias of about 38%. This bias occurs primarily during daytime. The root mean squared error (RMSE) between measured and VOM_{mlsc}-predicted CO_2 flux is approximately $9{\cdot}6 \times 10^{-6}$ mol m^{-2} s^{-1}, with a corresponding CV that is almost 106% (the solutions of the ensemble range between 97 and 114%). To benchmark whether the principle of vegetation optimality provides an accurate representation of the Douglas-fir stand, we continue our analysis and use measured CO_2 fluxes to calibrate the six VOM_{mlsc} parameters. This fitting results in an RMSE of about $6{\cdot}5 \times 10^{-6}$ mol m^{-2} s^{-1}, with a corresponding correlation coefficient of $r = 0{\cdot}81$ (Figure 5d). The VOM_{mlsc} parameter values that provide the best fit to the CO_2 flux data are MA = 0·65, $y_r = 2{\cdot}9$ m, $ce = 3{\cdot}89$, $me = 0{\cdot}98$, $m = 60$, and $J_{\max,t=0} = 100$ µmol m^{-2} s^{-1}. This parameter set provides a noticeably closer match to the observed CO_2 fluxes than the mean ensemble predictions of VOM_{mlsc} previously derived by optimality of NCP. The different dots are more closely grouped around the 1 : 1 regression line, and the bias towards higher CO_2 values is reduced to about 4%. Perhaps, most importantly, the optimized values of the structural parameters are also in much better agreement with their independently measured values.

DOI: 10.1002/eco

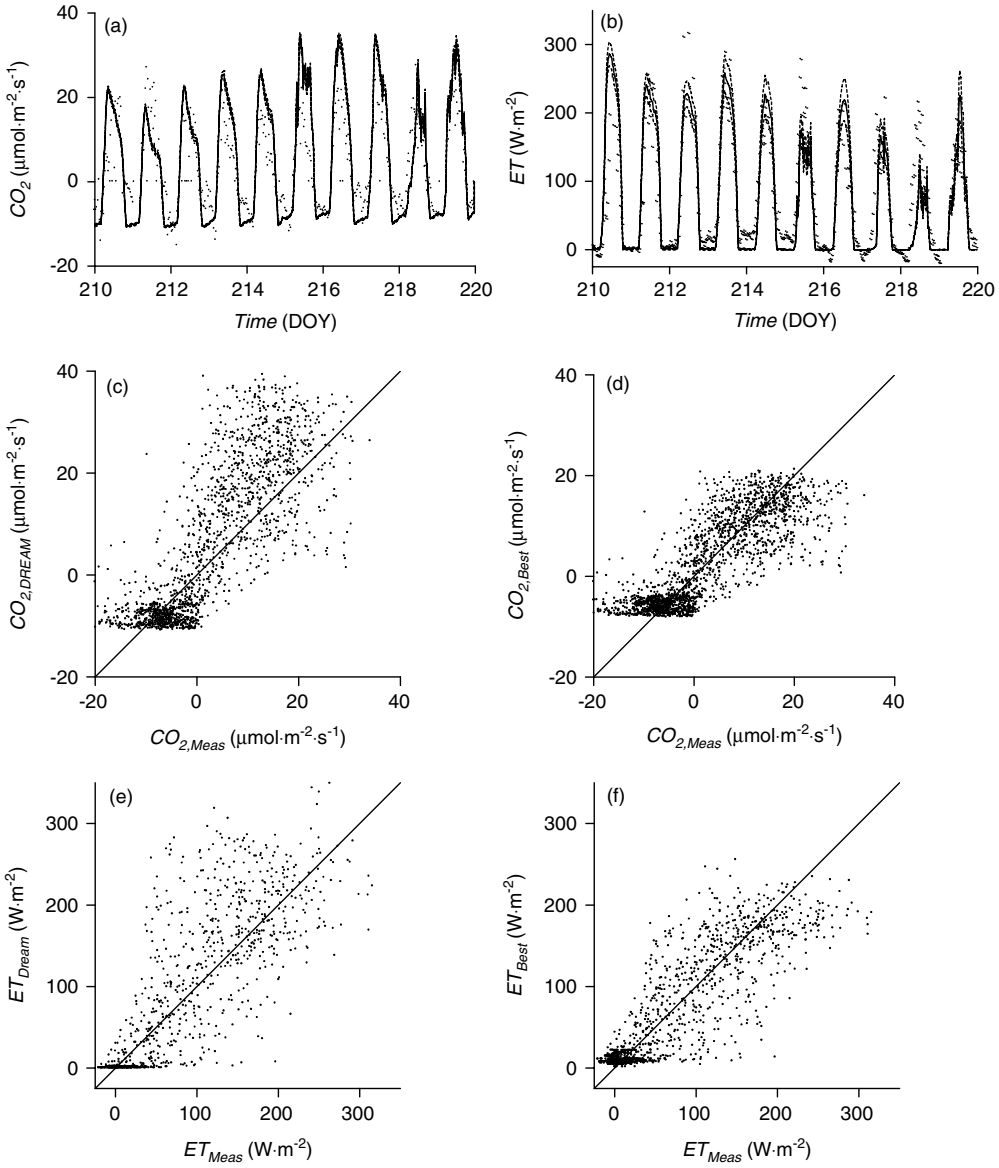

Figure 5. Comparison of measured half-hourly fluxes of CO_2 and ET against their VOM_{mlsc} modelled counterparts for the 1995 data set from the Speuldersbos. (a + b) Time series plots of DREAM-derived mean ensemble predictions (solid line) of (a) CO_2 (W m^{-2}) and (b) ET (W m^{-2}) fluxes and their respective observations (dots) for a period of 10 days; (c + e) mean ensemble VOM_{mlsc} predictions of half-hourly CO_2 and ET fluxes by optimality of NCP; (d + f) best attainable fit of VOM_{mlsc} to the measured half-hourly (d) CO_2 and (f) ET fluxes. This fit is derived by direct calibration against these respective fluxes using the DREAM stochastic search algorithm.

Figure 5e presents a two-dimensional scatter plot of mean ensemble VOM_{mlsc} predictions of half-hourly ET fluxes against their actual measurement. In all our calculations reported herein, the value of ET is computed as the sum of transpiration and soil evaporation. A relatively strong correlation ($r = 0{\cdot}84$) is found between measured and modelled ET fluxes with associated RMSE of about 51·6 W m^{-2}, and CV of ~68% (the ensemble ranges between 60 and 90%). The dots in Figure 5e generally follow the 1 : 1 regression line, resulting in a relatively small prediction bias of about 5%. If we use the ET data for calibration, the predictions of VOM_{mlsc} improve considerably (RMSE = 38·1 W m^{-2}, $r = 0{\cdot}87$), with a similar but now negative bias of $\sim -5\%$ (Figure 5f). This best VOM_{mlsc} parameterization uses MA = 0·93, $y_r = 3{\cdot}89$ m, $ce = 1{\cdot}47$, $me = 0{\cdot}86$, $m = 39$, and $J_{max,t=0} = 197$ µmol m^{-2} s^{-1}. These parameter values correspond well with their independently measured values. Yet, direct fitting to these ET data results in NCP values that are significantly lower than those derived previously in our first study. Indeed, NCP = −37 versus 129 mol m^{-2}, $\Sigma A_g = 127$ versus 162 mol m^{-2}, $\Sigma R_{ft} = 9{\cdot}1$ versus 3·0 mol m^{-2}, $\Sigma R_v = 137$ versus 19·1 mol m^{-2}, and $\Sigma R_r = 18{\cdot}0$ versus 12·7 mol m^{-2}. These results highlight two important observations. First, the optimized value of ΣA_g decreases with the increasing value of LAI. Seemingly, the costs of leaf respiration (R_l) are considerably larger than the benefits associated with growing more leafs and thus establishing a more dense vegetation cover. Second, the mathematical definition of NCP in VOM_{mlsc} needs to be revisited. If our definition of biological fitness was

DOI: 10.1002/eco

reasonable and our model a reasonable representation of reality, then calibrating VOM_{mlsc} to flux data would result in similar parameter values as when fitting against NCP. Yet, our study shows significant differences between these two different calibration approaches. Either the optimality hypothesis of NCP does not apply to the Douglas-fir plantation considered herein or the weighting of the different carbon costs and benefits that make up biological fitness is inaccurate, and subject to considerable uncertainty. Future work should revisit the definition of NCP and better quantify its individual carbon sources and sinks. Progress on this is only to be expected when the concept of vegetation optimality is applied to a wider range of ecosystems, and the strengths of numerical analysis and data collection continue to be merged.

Our results so far demonstrate that a substantially improved fit to the actual ET and CO_2 data can be obtained when these fluxes are used explicitly for calibration of the VOM_{mlsc} parameters. This finding questions the continued usefulness of NCP as single optimality criteria in forested, often managed ecosystem. The simultaneous use of multiple non-commensurable (optimality) criteria for ecohydrological parameter estimation and model evaluation has desirable advantages. However, as argued before, this approach requires site-specific eddy correlation measurements. These observations are not only expensive and time consuming but this approach also has limited applicability for predicting vegetation response outside current climate conditions.

To determine whether our simulation of soil moisture dynamics in the rooting zone represents the actual field data, our final evaluation of VOM_{mlsc} includes comparison of measured and simulated soil moisture data during a period of relative dryness. Water content was measured between day of year (DOY) 225–255 in 1995, with five TDR sensors vertically installed, measuring an integrated mean water content between 0 and 35 cm depth. Figure 6 presents the rainfall, pressure head and soil moisture content dynamics observed at our experimental site in the Speuldersbos during the year 1995. The top panel depicts the measured rainfall hyetograph (Figure 6a), whereas the bottom two panels plot time series of mean ensemble simulated pressure head (Figure 6b), and root-zone moisture content (Figure 6c) both at 15 cm depth. In these bottom two graphs, the dark line denotes the evolution of the DREAM-derived mean ensemble prediction, whereas the dotted lines represent the associated 95% prediction uncertainty ranges. The dots in Figure 6c represent the mean TDR measurement with error bars defining the spatial variability among the five different probes. Although the values of the maximum rooting depth estimated by optimality of NCP are substantially smaller than those observed in the field, simulated soil moisture dynamics in the upper part of the rooting zone is in good agreement with corresponding TDR measurements at the same experimental site ($r = 0{\cdot}74$). This is a promising result, considering the fact that no explicit information in VOM_{mlsc} is used about the soil moisture status at the lower boundary condition.

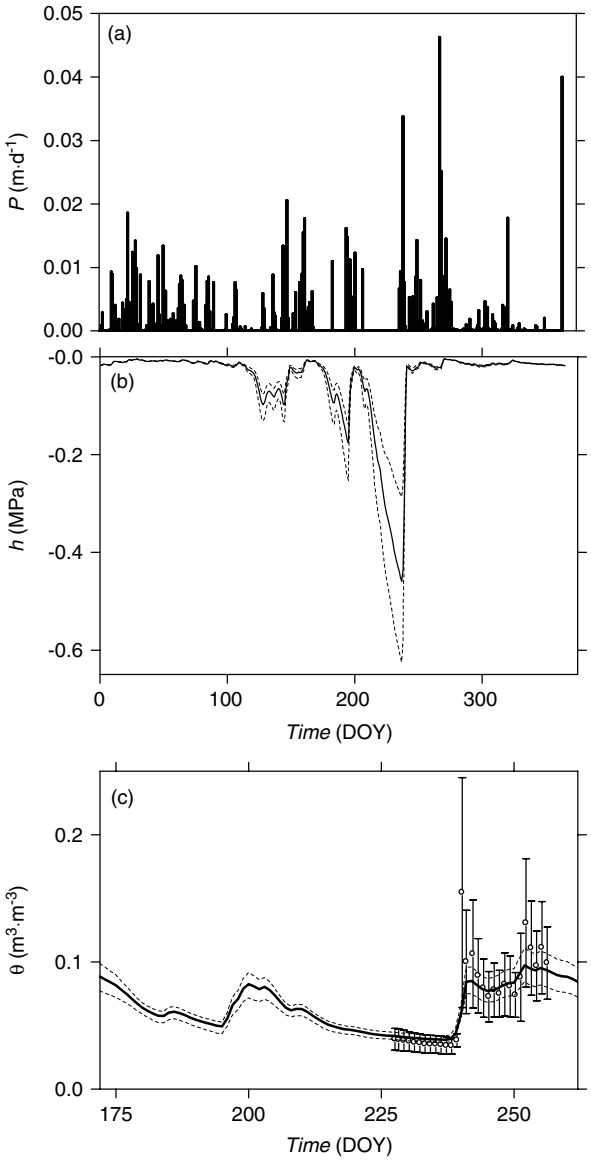

Figure 6. Comparison of measured and VOM_{mlsc} modelled time series of pressure head and soil moisture dynamics in the top part of the rooting zone using the 1995 data set from the Speuldersbos. (a) Rainfall hyetograph (P, m d^{-1}), (b) mean (thick line), minimum and maximum (hair lines) values of the simulated pressure head (h, MPa) in the rooting zone, and (c) water content (θ, m^3 m^{-3}) dynamics at the 10 cm depth. The various lines represent the mean (thick), minimum, and maximum (hair) simulated soil moisture contents of the DREAM ensemble of solutions. Circles depict measured soil moisture values from five vertically installed TDR sensors between 0 and 35 cm depth. Bars represent standard deviations of the soil moisture measurements. DOY is an abbreviation of day of the year.

DISCUSSION AND CONCLUSIONS

Ecohydrological models are increasingly being used to study stomatal behaviour and predict the exchange of CO_2 and H_2O between vegetation and the ambient atmosphere. The goals of this study were twofold. First, we have introduced a multi-layer canopy model coupling soil moisture dynamics with ecophysiological

DOI: 10.1002/eco

gas exchange and photosynthesis. This model, referred to as VOM_{mlsc}, is based on the original single big-leaf VOM of Schymanski (2007) and Schymanski *et al.* (2007), but includes a multi-layer canopy model to better represent vegetation properties and dynamics at high LAI, and a time-varying throughfall fraction to better represent rainfall interception. In the second part of this article we have presented a stochastic optimality approach to ecohydrological parameter estimation. While current optimality approaches typically focus on finding a single best combination of parameter values, our inverse approach is especially designed to estimate a distribution of 'optimal' parameter values. Such distribution contains important diagnostic information about the model and optimality criteria used. We have used the DREAM MCMC to efficiently sample the parameter space and illustrate the advantages of our stochastic approach. We have tested and evaluated VOM_{mlsc} using data from a Douglas-fir stand in The Netherlands and conclude that:

1. The stochastic optimality approach considered herein results in a distribution of 'optimal' parameter values that provide important diagnostic information about the model and optimality criteria used. Our study demonstrates significant dispersion in vegetation properties and dynamics from ecohydrological optimality of NCP. The range of acceptable solutions found in our study suggests that many different plant species can be found that lead to very similar (optimal) values of NCP, describing similar biological fitness.
2. VOM_{mlsc} was shown to be of appropriate complexity. Most static and dynamic vegetation properties in VOM_{mlsc} are warranted by optimality of NCP. The principle of vegetation optimality, however, is inadequate to warrant the identification of the water use efficiency relationship. This relationship exhibits significant dispersion and therefore needs to be simplified using only a single calibration parameter.
3. The inference uncertainty of the water use relationship translates into large prediction uncertainty of simulated evapotranspiration. Simulated CO_2 fluxes show considerable smaller uncertainty by optimality against NCP.

Comparison of measured and VOM_{mlsc} modelled fluxes of evapotranspiration and carbon dioxide uptake, and root-zone soil moisture demonstrate that:

4. VOM_{mlsc} predictions of half-hourly fluxes of plant evapotranspiration (ET) and carbon dioxide (CO_2) uptake derived by optimality of NCP and without site-specific data depart considerably from their observed values using the eddy correlation measurement technique.
5. A much closer fit to the measured ET and CO_2 fluxes at the Douglas-fir stand is possible when these respective fluxes are used explicitly for calibration of VOM_{mlsc}. The fit to CO_2 data improved from $9{\cdot}6 \times 10^{-6}$ μmol m^{-2} s^{-1} to $6{\cdot}5 \times 10^{-6}$ μmol m^{-2} s^{-1}, whereas the RMSE for ET reduces from 51·6 W m^{-2} to 38·5 W m^{-2}. Besides this significant improvement in fit, the optimized values of the structural parameters also show much better agreement with their independently measured values. These findings not only question the validity of VOM for our Douglas-fir plantation but also challenge the definition of biological fitness used herein. The weighting scheme used to aggregate the different carbon costs and benefits into a single NCP scalar requires important rethinking. The costs of leaf respiration and water transport to plant roots are particularly difficult to quantify. Site-specific flux data are required to unravel and quantify the various processes that together define biological fitness.
6. VOM_{mlsc} predictions of root-zone soil moisture content compare relatively well with measured water content values derived from vertically installed TDR probes.

The use of NCP is based on the assumption that vegetation adapts itself optimally to the existing environmental conditions. At first glance, VOM_{mlsc} simulations of CO_2 uptake and plant transpiration compare reasonably well with their respective observed fluxes at the experimental site. This is an encouraging result because these two fluxes have not been used for parameter fitting and VOM_{mlsc} is developed specifically for natural conditions. Hence, our ecosystem is human-altered and grows a Douglas-fir plantation.

Unfortunately, some disturbing differences become apparent when closely inspecting the various results. The various fluxes calculated with VOM_{mlsc} not only depart from their actual measured values but the optimized ecohydrological parameters also deviate considerably from their independently measured values at the Douglas-fir plantation. For instance, the maximum rooting depth at the experimental site of about 2·5 m (Tiktak and Bouten, 1994) is considerably larger than the DREAM-derived range of y_r between 0·5 and 0·7 m. Real-world canopies typically develop their rooting system in such a way that they can adapt quickly and survive severe drought or other difficult conditions such as nutrient shortages or poor soil fertility (e.g. Holtkamp *et al.* 2008). The DREAM-optimized range of MA between 0·96 and 1·00 is considerably higher than its value of approximately 0·83 derived from calibration of a single-layer rainfall interception model using detailed measurements of forest canopy storage (Vrugt *et al.*, 2003a). Finally, observed LAI values range between 7·8 and 10·5 m^2 m^{-2} (Dekker *et al.*, 2000), whereas DREAM incorrectly predicts the LAI to vary between 1·6 and 3·4 m^2 m^{-2}. These differences are substantial and question the usefulness of VOM to predict vegetation properties and dynamics for our Douglas-fir plantation.

Besides some disturbing differences in observed and calibrated parameter values, optimality of NCP also results in cumulative yearly transpiration amounts that exhibit too much variation. The computed range between 0·31 and 0·50 m is unrealistically large for our experimental field site. In The Netherlands cumulative yearly

DOI: 10.1002/eco

transpiration amounts of grasses and forests will generally not differ more than 20% (Makkink, 1957). Our DREAM ensemble of solutions, however, predicts a much larger difference between 0·31 and 0·50 m in yearly evapotranspiration amounts. This difference is simply too large and inconsistent with available observations. Photosynthetic CO_2 uptake fluxes (A_g), on the contrary, exhibit a much smaller yearly variation with cumulative amounts ranging between 98 and 112 mol m^{-2}. This is consistent with the vegetation optimality theory of Cowan and Farquhar (1977) that predicts optimal CO_2 uptake with varying differences in ET fluxes. Finally, the principle of vegetation optimality did not favour a particular water use strategy, and is therefore inadequate to reliably estimate the water use efficiency relationship. Future work should be focused on improving the different carbon costs and benefits describing biological fitness, particularly those related to leaf respiration and water transport.

To benchmark these results, we performed two final MCMC trails with DREAM, and calibrated VOM_{mlsc} using time series of observed half-hourly fluxes of ET and CO_2 uptake at the experimental site during the year 1995. Significant improvements in the fit of the calibration data and optimized values of the parameters can be achieved when VOM_{mlsc} was fitted directly against the corresponding eddy covariance data. For instance, explicit use of ET (CO_2) flux data for calibration of VOM_{mlsc} resulted in optimized values of y_r of 3·9 (2·9)m. The marginal distribution of MA ranged between 0·65 and 0·93 with corresponding value of LAI that varied between 7·2 and 7·8 m^2 m^{-2}. These optimized values are much closer to their observed counterparts. These findings not only inspire confidence in VOM_{mlsc} ability to accurately represent the Douglas-fir plantation but also question the correctness of the current weights used to aggregate the various carbon costs and benefits into a single NCP scalar.

Direct measurements of $J_{max\,25,0}$ have been made at eight different forest sites throughout the world, and these observations range between 52 and 225 μmol m^{-2} s^{-1} (Wang *et al*., 2007). Our time-dependent estimate of $J_{max\,25,0}$ varies from 125 μmol m^{-2} s^{-1} in winter to approximately 300 μmol m^{-2} s^{-1} in summer, with associated mean canopy value of $J_{max\,25,0}$ that ranges between 79 μmol m^{-2} s^{-1} in winter and 185 μmol m^{-2} s^{-1} in summer. Unfortunately, we do not have any knowledge of the water use efficiency parameters *ce* and *me*, except that significant correlations are found between these respective parameters, and modelled fluxes of transpiration and photosynthetic CO_2 uptake.

The optimized parameters not only demonstrated a much closer agreement with their independently observed values, VOM_{mlsc} predicted fluxes of ET and CO_2 uptake corresponded noticeably better with their respective observations. For instance, the RMSE of the model fit to CO_2 data improved from $9{\cdot}6 \times 10^{-6}$ μmol m^{-2} s^{-1} to $6{\cdot}5 \times 10^{-6}$ μmol m^{-2} s^{-1}. This improvement in fit is significant considering that the measurement error of the CO_2 flux data is about 3·2 μmol m^{-2} s^{-1} (Richardson *et al*., 2008). When measured ET fluxes were explicitly used for parameter inference then the RMSE of the model fit to this data decreased from 51·6 W m^{-2} to 38·5 W m^{-2}. This is a substantial error reduction, particularly when compared to the measurement error of ET flux data, which is on the order of 21 W m^{-2} (Dekker *et al*., 2000).

The significant dispersion in vegetation characteristics and dynamics, the mismatch between measured and modelled H_2O and CO_2 fluxes, and the discrepancy between optimized and measured values of the VOM_{mlsc} parameters (discussed above), question the continued usefulness of NCP as main optimality criteria for ecohydrological parameter estimation. Our results suggest that detailed field data are necessary to better constrain VOM_{mlsc} parameter uncertainty, and force the model predictions to closer match the actual observed fluxes of plant transpiration and CO_2 assimilation. Specifically, we advocate the use of a hybrid multi-criteria approach for ecohydrological parameter estimation and model evaluation that combines the strengths of optimality modelling and field data. The resulting parameter estimation problem can be solved using multi-criteria (Pareto) optimization. An example of this approach within the context of long distance bird migration of passerine birds was recently presented in Vrugt *et al*. (2007). The optimized flight routes jointly minimizing migration flight time and daily energy-use correspond well with historical migration pathways of Willow Warblers established from extensive ringing recoveries.

The results for the first case study presented herein are contingent upon the exact definition of the fitness function used to derive the model parameters. In our analysis, the actual values of the rooting depth and LAI were underestimated. Somehow, the costs for a deeper root system and higher LAI were exceedingly large and the potential benefits insufficient to warrant such development. Explicit use of eddy covariance data resulted in more realistic estimates of the maximum rooting depth and LAI. Measured ET and CO_2 fluxes provide the necessary information to help disentangle the different carbon costs and benefits associated with NCP. Continued application of VOM_{mlsc} to a wide range of different ecosystems will help to better understand the strengths and weaknesses of VOM. In this research, stochastic search algorithms are of imminent importance to appropriately treat uncertainty and spatial variability, and infer a range of plausible solutions given the optimality criteria or data used.

ACKNOWLEDGMENTS

We acknowledge the many constructive and useful comments of the reviewers that helped us to improve our manuscript. In particular, we thank Stan Schymanski for his valuable comments and suggestions regarding the development of VOM_{mlsc}, and Norman Bean for help with the figures. The first author is sponsored by a High

DOI: 10.1002/eco

Potential Program of Utrecht University, and the second author is supported by a J. Robert Oppenheimer Fellowship of the Los Alamos National Laboratory Postdoctoral Program. The source code of DREAM and VOM_{mlsc} used throughout this article is written in MATLAB and can be obtained from the second author (jasper@uci.edu) upon request.

REFERENCES

Acock B, Charles-Edwards DA, Fitter DJ, Hand DW, Ludwig J, Warren-Wilson J and Withers AC, 1978. The contribution of leaves from different levels within a tomato crop to canopy net photosynthesis: an experimental examination of two canopy models. *Journal of Experimental Botany* **29**: 815–827.

Black TA, Gardner WR, Thurtell GW. 1969. The prediction of evaporation, drainage and soil water storage for a bare soil. *Soil Science Society of America Proceedings* **33**: 655–660.

Britton CM, Dodd JD. 1976. Relationships of photosynthetically active radiation and shortwave irradiance. *Agricultural Meteorology* **17**: 1–7.

Brolsma RJ, Bierkens MFP. 2007. Groundwater–soil water-vegetation dynamics in a temperate forest ecosystem along a slope. *Water Resources Research* **43**(1): W01414.

Cowan IR, Farquhar GD. 1977. Stomatal function in relation to leaf metabolism and environment. In *Integration of Activity in the Higher Plant*, Jennings DH (ed.). Cambridge University Press: Cambridge; 471–505.

Dekker SC, Bouten W, Schaap MG. 2001. Analysing forest transpiration model errors with artificial neural networks. *Journal of Hydrology* **246**: 197–208.

Dekker SC, Bouten W, Verstraten JM. 2000. Modelling forest transpiration from different perspectives. *Hydrological Processes* **14**(2): 251–260.

Duursma RA, Marshall JD, Robinson AP. 2003. Leaf area index inferred from solar beam transmission in mixed conifer forests on complex terrain. *Agricultural and Forest Meteorology* **118**(3–4): 221–236.

Eagleson PS. 1978. Climate, soil, and vegetation; 6, dynamics of the annual water balance. *Water Resources Research* **14**(5): 749–764.

Farquhar GD, von Caemmerer S. 1982. Modeling of photosynthetic response to environmental conditions. In *Encyclopedia of Plant Physiology New Series*, Lange PNO, Osmond C, Ziegler H (eds). Springer-Verlag: Berlin; 550–587.

Freijer JI, de Jonge H, Bouten W, Verstraten JM. 1997. Assessing mineralization rates of petroleum hydrocarbons in soils in relation to environmental factors and experimental scale. *Biodegradation* **7**(6): 487–500.

Gelman A, Rubin DB. 1992. Inference from iterative simulation using multiple sequences. *Statistical Science* **7**: 457–472.

Givnish TJ. 2002. Adaptive significance of evergreen vs. deciduous leaves: solving the triple paradox. *Silva Fennica* **36**(3): 703–743.

Holtkamp R, Kardol P, van der Wal A, Dekker SC, van der Putten WH and de Ruiter PC. 2008. Soil food web structure during ecosystem development after land abandonment. *Applied Soil Ecology* **39**(1): 23–34.

Jackson RB, Canadell J, Ehleringer JR, Mooney HA, Sala OE and Schulze ED. 1996. A global analysis of root distributions for terrestrial biomes. *Oecologia* **108**(3): 389–411.

Kerkhoff AJ, Martens SN, Milne BT. 2004. An ecological evaluation of Eagleson's optimality hypotheses. *Functional Ecology* **18**(3): 404–413.

Kleidon A. 2007. Optimized stomatal conductance and the climate sensitivity to carbon dioxide. *Geophysical Research Letters* **34**(14): L14709.

Kull O. 2002. Acclimation of photosynthesis in canopies: models and limitations. *Oecologia* **133**(3): 267–279.

Makela A, Berninger F, Hari P. 1996. Optimal control of gas exchange during drought: theoretical analysis. *Annals of Botany* **77**(5): 461–467.

Makkink GF. 1957. Testing the Penman formula by means of lysimeters. *International Journal of Water Engineering* **11**: 277–288.

Medlyn BE, Dreyer E, Ellsworth D, Forstreuter M, Harley PC, Kirschbaum MUF, Le Roux X, Montpied P, Strassemeyer J, Walcroft A, Wang K and Loustau D. 2002. Temperature response of parameters of a biochemically based model of photosynthesis. II. A review of experimental data. *Plant Cell and Environment* **25**(9): 1167–1179.

Misson L, Tu KP, Boniello RA, Goldstein AH. 2006. Seasonality of photosynthetic parameters in a multi-specific and vertically complex forest ecosystem in the Sierra Nevada of California. *Tree Physiology* **26**(6): 729–741.

Niinemets U, Oja V, Kull O. 1999. Shape of leaf photosynthetic electron transport versus temperature response curve is not constant along canopy light gradients in temperate deciduous trees. *Plant Cell and Environment* **22**(12): 1497–1513.

Mualem Y. 1976. A new model predicting the hydraulic conductivity of unsaturated porous media. *Water Resources Research*. **12**: 513–522.

Reynolds JF, Chen J. 1996. Modelling whole-plant allocation in relation to carbon and nitrogen supply: coordination versus optimization: opinion. *Plant and Soil* **185**: 65–74.

Richardson AD, Mahecha MD, Falge E, Kattge J, Moffat AM, Papale D, Reichstein M, Stauch VJ, Braswell BH, Churkina G, Kruijt B and Hollinger DY. 2008. Statistical properties of random CO_2 flux measurement uncertainty inferred from model residuals. *Agricultural and Forest Meteorology* **148**(1): 38–50.

Rodriguez-Iturbe I, D'Odorico P, Porporato A, Ridolfi L. 1999. On the spatial and temporal links between vegetation, climate, and soil moisture. *Water Resources Research* **35**(12): 3709–3722.

Roxburgh SH, Berry SL, Buckley TN, Barnes B, Roderick ML. 2005. What is NPP? Inconsistent accounting of respiratory fluxes in the definition of net primary production. *Functional Ecology* **19**(3): 378–382.

Schymanski SJ. 2007. *Transpiration as the leak in the carbon factory: a model of self-optimising vegetation*. PhD thesis, University of Western Australia: Perth, Australia; 234.

Schymanski SJ, Roderick ML, Sivapalan M, Hutley LB, Beringer J. 2007. A test of the optimality approach to modelling canopy properties and CO_2 uptake by natural vegetation. *Plant Cell and Environment* **30**(12): 1586–1598.

Schymanski SJ, Roderick ML, Sivapalan M, Hutley LB, Beringer J. 2008. A canopy-scale test of the optimal water-use hypothesis. *Plant Cell and Environment* **31**: 97–111.

Schymanski SJ, Sivapalan M, Roderick ML, Hutley LB, Beringer J. 2009. An optimality-based model of the dynamic feedbacks between natural vegetation and the water balance. *Water Resources Research* **45**: W01412.

Spitters CJT, Toussaint HAJM, Goudriaan J. 1986. Seperating the diffuse and direct component of global radiation and its implications for modelling canopy photosynthesis. *Agricultural and Forest Meteorology* **38**: 217–229.

Sutherland WJ. 2005. The best solution. *Nature* **435**: 569–569.

Thornley JHM. 2002. Instantaneous canopy photosynthesis: analytical expressions for sun and shade leaves based on exponential light decay down the canopy and an acclimated non-rectangular hyperbola for leaf photosynthesis. *Annals of Botany* **89**(4): 451–458.

Tiktak A, Bouten W. 1994. Soil water dynamics and long-term water balances of a Douglas-fir stand in the Netherlands. *Journal of Hydrology* **156**: 265–283.

van Genuchten MT. 1980. A closed form equation for predicting the hydraulic conductivity of unsaturated soils. *Soil Science Society of America Journal* **44**: 892–898.

Van Wijk MT, Dekker SC, Bouten W, Kohsiek W, Mohren GMJ. 2001. Simulation of carbon and water budgets of a Douglas-fir forest. *Forest Ecology and Management* **145**(3): 229–241.

Vrugt JA, Dekker SC, Bouten W. 2003a. Identification of rainfall interception model parameters from measurements of throughfall and forest canopy storage. *Water Resources Research* **39**(9): 1251 DOI: 10.1029/2003WR002013.

Vrugt JA, Gupta HV, Bouten W, Sorooshian S. 2003b. A shuffled complex evolution metropolis algorithm for optimization and uncertainty assessment of hydrologic model parameters. *Water Resources Research* **39**(8): 1201.

Vrugt JA, ter Braak CJF, Clark MP, Hyman JM, Robinson BA. 2008. Treatment of input uncertainty in hydrologic modelling: doing hydrology backward with Markov chain Monte Carlo simulation. *Water Resources Research* **44**(W00B09): DOI: 10.1029/2007WR006720).

Vrugt JA, ter Braak CJF, Diks CGH, Higdon D, Robinson BA and Hyman JM. 2009a. Accelerating Markov chain Monte Carlo simulation by differential evolution with self-adaptive randomized subspace sampling. *International Journal of Nonlinear Sciences and Numerical Simulation* **10**(3): 273–290.

Vrugt JA, ter Braak CJF, Gupta HV, Robinson BA. 2009b. Equifinality of formal (DREAM) and informal (GLUE) Bayesian approaches in hydrologic modelling? *Stochastic Environmental Research and Risk Assessment* **1–16**: 1011–1026 DOI: 10.1007/s00477-008-0274-y.

Vrugt JA, van Belle J, Bouten W. 2007. Pareto front analysis of flight time and energy use in long-distance bird migration. *Journal of Avian Biology* **38**(4): 432–442.

Wang YP, Baldocchi D, Leuning R, Falge E, Vesala T. 2007. Estimating parameters in a land-surface model by applying nonlinear inversion to eddy covariance flux measurements from eight FLUXNET sites. *Global Change Biology* **13**(3): 652–670.

Wright IJ, Reich PB, Westoby M, Ackerly DD, Baruch Z, Bongers F, Cavender-Bares J, Chapin T, Cornelissen JHC, Diemer M, Flexas J, Garnier E, Groom PK, Gulias J, Hikosaka K, Lamont BB, Lee T, Lee W, Lusk C, Midgley JJ, Navas ML, Niinemets U, Oleksyn J, Osada N, Poorter H, Poot P, Prior L, Pyankov VI, Roumet C, Thomas SC, Tjoelker MG, Veneklaas EJ, Villar R. 2004. The worldwide leaf economics spectrum. *Nature* **428**(6985): 821–827.

DOI: 10.1002/eco